Jets at Hadron Colliders

Nigel Glover

IPPP, University of Durham

CTEQ, Rhodes, July 2006

Hard processes in Hadron-Hadron collisions

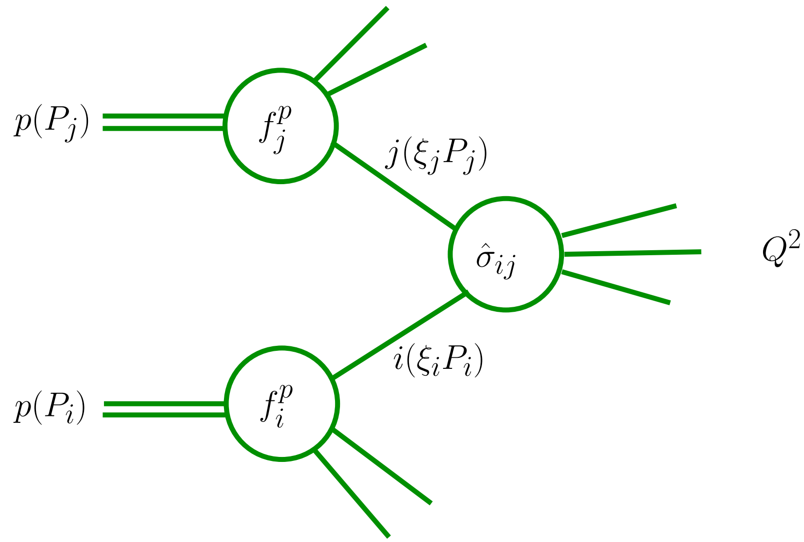

$$\sigma(Q^2) = \sum_{i,j} \left[\hat{\sigma}_{ij}(\alpha_s(\mu^2), \mu_R^2/Q^2, \mu_F^2/Q^2) \otimes f_i^p(\mu_F^2) \otimes f_j^p(\mu_F^2)\right]$$

- **partonic cross sections** σ_{ij}
- **parton distributions** f_i
- **renormalization/factorization scale** μ_R/μ_F

Jet Physics in SM and Beyond

- ✓ SM Physics **with** jets
  jet production $\Rightarrow$ QCD at large energy scales
- ✓ SM Physics **of** jets
  jet structure $\Rightarrow$ QCD at small energy scales
- ✓ QCD and jets are **the key** to New Physics
  - ✓ new physics is likely to be born in a QCD process
  - ✓ new physics often results in jets in final states
  - ✓ most of time QCD is major backgound

Theoretically, QCD is a challenge

- ✗ at large energies where α_s is small
- ✗ at low energy scales where it is large

Experimentally, jets are a challenge

- ✗ suffer large uncertainties - algorithm, calorimeters, $\ldots$
- ✗ contaminate other tools such as γ, e, $E_T^{miss}, \ldots$

Typical jet event

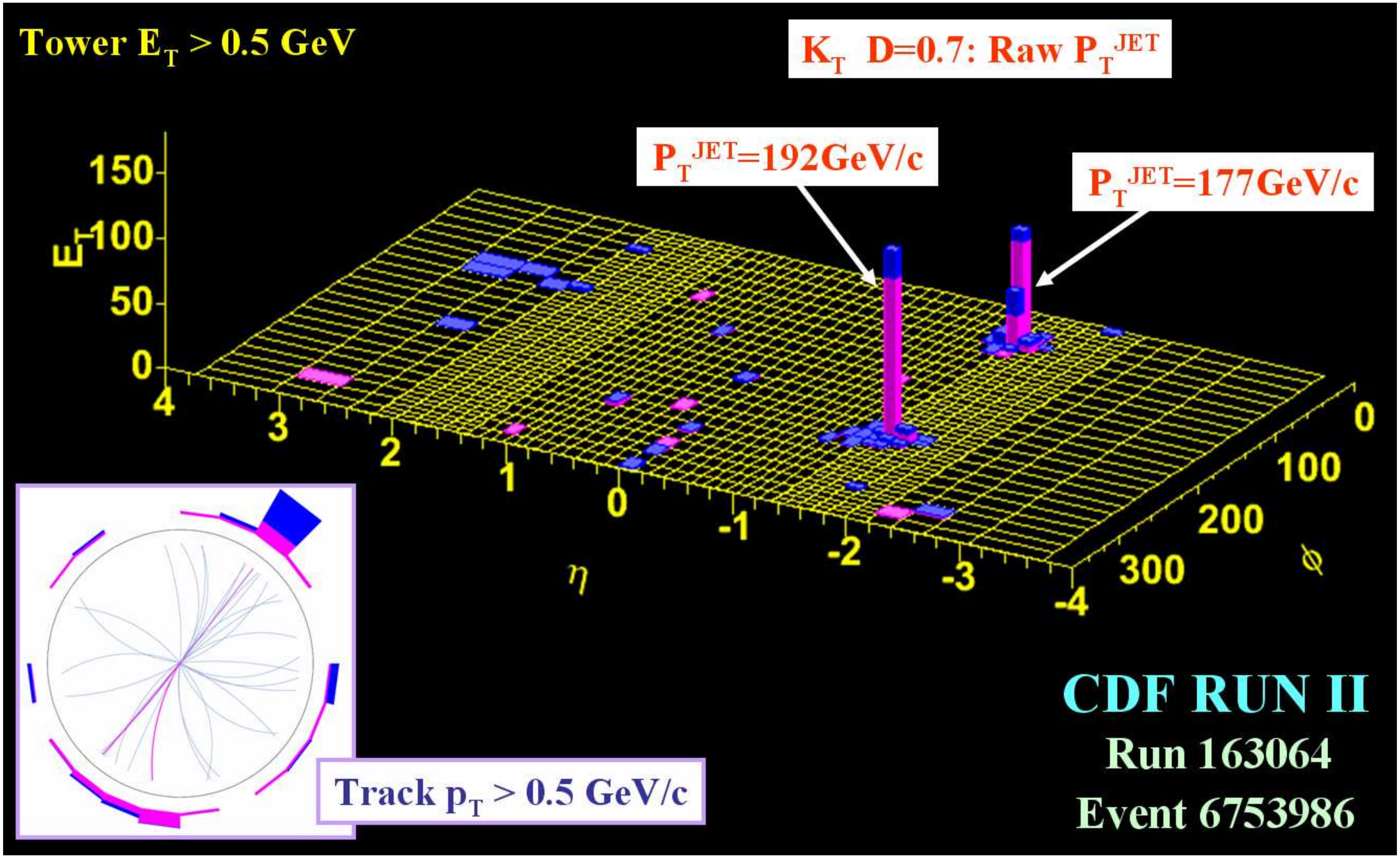

Kinematics in Hadronic Collisions

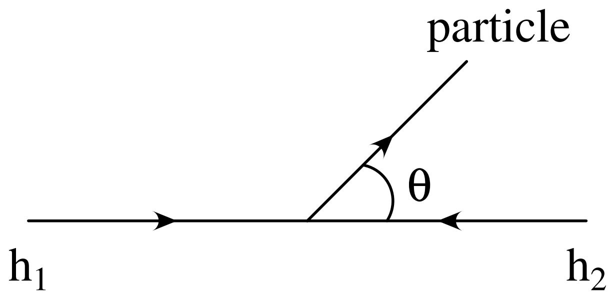

- **Rapidity (y)**

$$y \equiv \frac{1}{2}\ln\left(\frac{E+p_z}{E-p_z}\right) = \frac{1}{2}\ln\left(\frac{1+\beta\cos\theta}{1-\beta\cos\theta}\right)$$

- **Pseudo-rapidity η**
  In the high energy limit, $\beta \to 1$ or $m \to 0$ then,

$$\eta \equiv \frac{1}{2}\ln\left(\frac{1+\cos\theta}{1-\cos\theta}\right) = -\ln\left(\tan\left(\theta/2\right)\right)$$

Kinematics in Hadronic Collisions

- **Transverse energy** E_T

$$E_T^2 = m^2 + p_x^2 + p_y^2 = m^2 + p_T^2 = E^2 - p_z^2$$

$$\begin{aligned} p_T &= p\sin\theta \\ p_z &= E\tanh y = E_T\sinh y \\ E &= E_T\cosh y \end{aligned}$$

For massless particles, $E_T \to p_T$

- **Invariant Mass**

$$M_{12}^2 = (p_1 + p_2)^2 = m_1^2 + m_2^2 + 2(E_1 E_2 - \vec{p_1}\cdot\vec{p_2})$$

For massless particles,

$$M_{12}^2 \to 2E_{T1}E_{T2}(\cosh\Delta\eta - \cos\Delta\phi)$$

Typical $2 \to 2$ scattering event

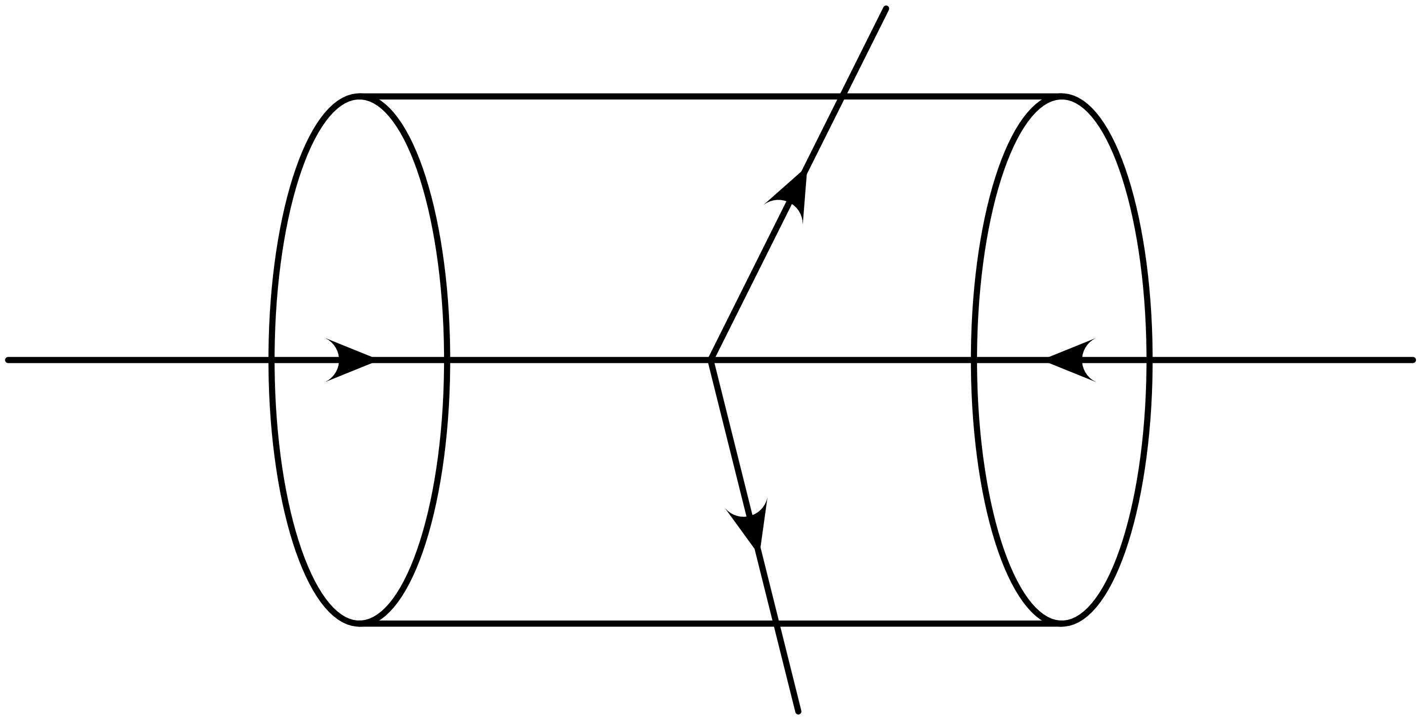

Two clear jets, separated in azimuth by π radians

Kinematics for $2 \to 2$ scattering

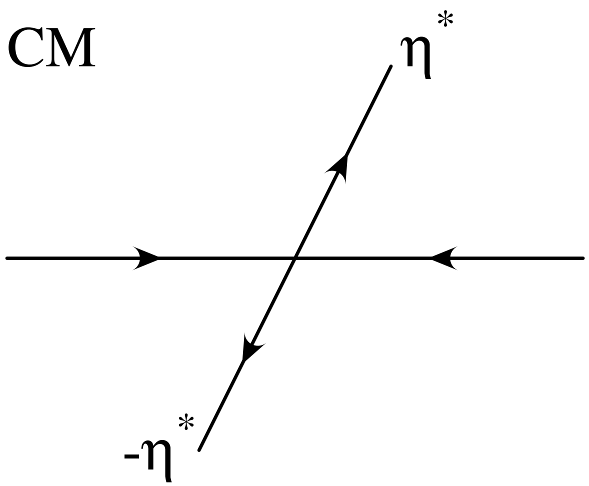

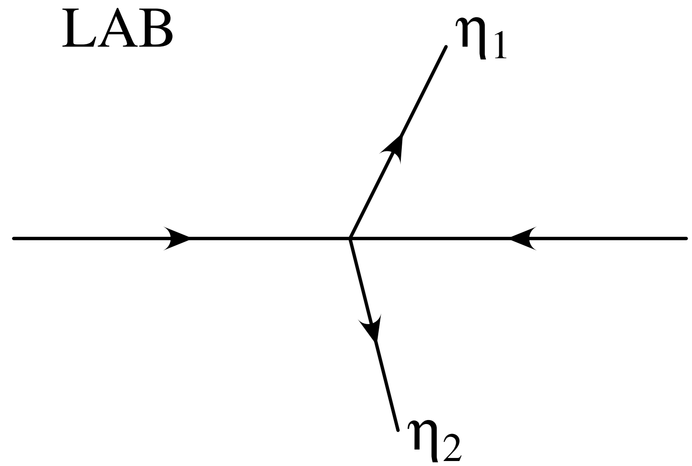

$$\eta^* = \frac{1}{2}(\eta_1 - \eta_2), \qquad \eta^{\text{boost}} = \frac{1}{2}(\eta_1 + \eta_2), \qquad \eta_{\text{LAB}} = \eta^* + \eta^{\text{boost}}$$

$$E_{T1} = E_{T2}$$

Kinematics for $2 \to 2$ scattering

To orient ourselves in the $\eta_1 - \eta_2$ plane, we first focus on the allowed phase space in terms of η_1 and η_2. At lowest order, the jet pseudorapidities are directly related to the parton fractions by

$$x_1 = \frac{E_T}{\sqrt{s}} \left(e^{\eta_1} + e^{\eta_2}\right), \qquad x_2 = \frac{E_T}{\sqrt{s}} \left(e^{-\eta_1} + e^{-\eta_2}\right).$$

Since the momentum fraction cannot exceed unity, we find,

$$-\log\left(\frac{2 - x_T \exp(-\eta_1)}{x_T}\right) < \eta_2 < \log\left(\frac{2 - x_T \exp(\eta_1)}{x_T}\right),$$

and,

$$|\eta_1| < \cosh^{-1}\left(\frac{1}{x_T}\right),$$

where $x_T = 2E_T/\sqrt{s}$ and $x_T^2 < x_1 x_2 < 1$.

Exercise: prove these boundaries on η_1 and η_2

Phase space for $2 \to 2$ scattering

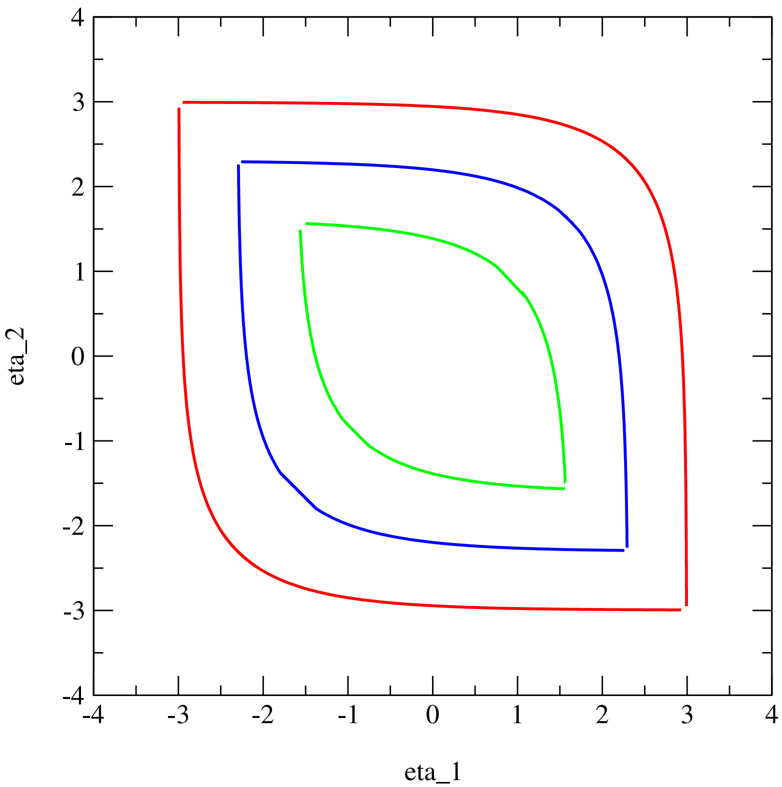

Phase space boundary for jets of E_T = 100, 200 and 400 GeV at $\sqrt{s} = 2$ TeV

- As E_T increases, the allowed phase space shrinks.
- for $\eta_1 \sim -\eta_2$, the energy of the particles approaches the beam energy
- for $\eta_1 \sim +\eta_2$, $M_{12}^2 \sim 4E_T^2$

Phase space for $2 \to 2$ scattering

Kinematics determined by E_T, η_1 and η_2.

$\Rightarrow$ observe triple differential cross section $d^3\sigma/dE_T d\eta_1 d\eta_2$

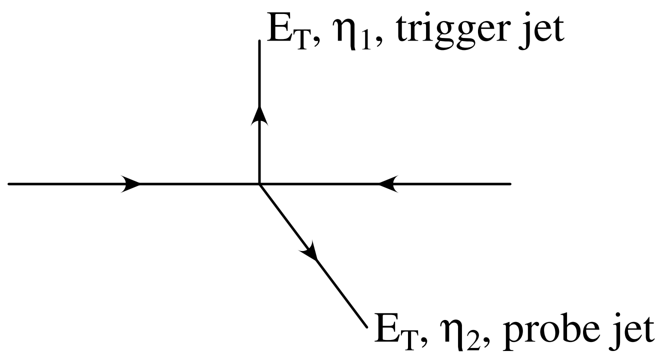

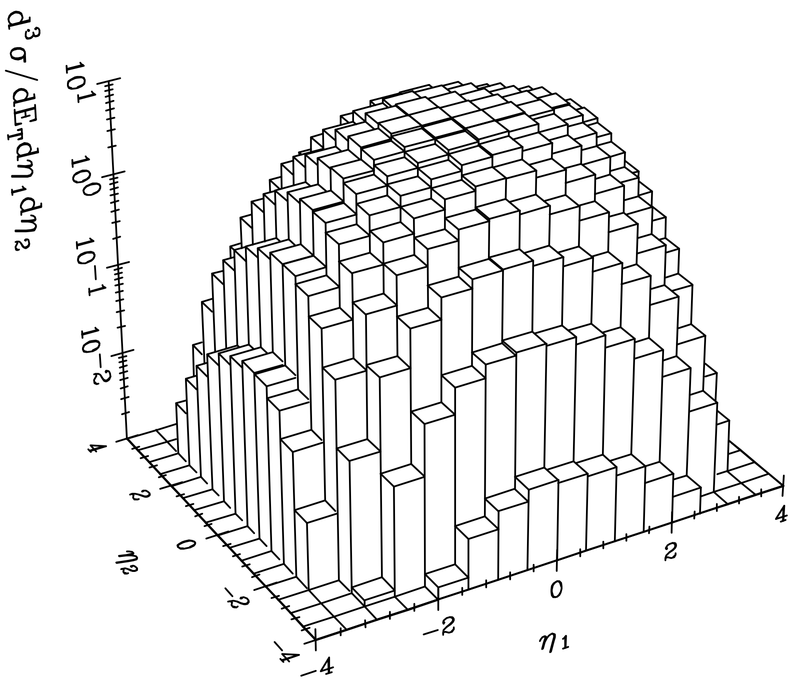

Many different observables;

- Single jet inclusive E_T distribution
- Same-side to Opposite-side jet ratio

Cross section for jet production

In terms of the natural kinematic variables, the cross section for two jet production at leading order is given by

$$\frac{d^3\sigma}{dE_T d\eta_1 d\eta_2} = \frac{1}{8\pi} \sum_{ij} x_1 f_i(x_1, \mu_F)\, x_2 f_j(x_2, \mu_F)$$

$$\times \frac{\alpha_s^2(\mu_R)}{E_T^3} \frac{|\mathcal{M}_{ij}(\eta^*)|^2}{\cosh^4 \eta^*},$$

where

- $f_i(x, \mu_F)$ ($i = g, q, \bar{q}$) represents the density of parton i in the proton at factorisation scale μ_F
- $|\mathcal{M}_{ij}|^2$ is the lowest order squared matrix element for $ij \to 2$ partons summed and averaged over initial and final state spins and colours.
- For parton-parton scattering, many subprocesses contribute; $qq \to qq$, $q\bar{q} \to q\bar{q}$, $qg \to qg$, $gg \to gg$, etc etc;

Spin averaged lowest order matrix elements

The matrix elements for

$$a(p_1) + b(p_2) \longrightarrow c(p_3) + d(p_4)$$

averaged (summed) over initial (final) state colours and spins

Process	$\sum \lvert M\rvert^2/g^4$
$q\bar{q} \to q'\bar{q}'$	$\frac{4}{9}\frac{u^2+t^2}{s^2}$
$q\bar{q} \to q\bar{q}$	$\frac{4}{9}\left(\frac{u^2+t^2}{s^2}+\frac{u^2+s^2}{t^2}\right)-\frac{8}{27}\frac{u^2}{st}$
$qg \to qg$	$\frac{u^2+s^2}{t^2}-\frac{4}{9}\frac{u^2+s^2}{su}$
$gg \to gg$	$\frac{9}{2}\left(3-\frac{ut}{s^2}-\frac{us}{t^2}-\frac{ts}{u^2}\right)$

where $s=(p_1+p_2)^2$, $t=(p_1-p_3)^2$ and $u=(p_2-p_3)^2$ are the Mandelstam variables.

Spin averaged lowest order matrix elements

The matrix elements for other processes are obtained by crossing - e.g.

$$\sum |M|^2_{q\bar{q}' \to q\bar{q}'}(s,t,u) = \sum |M|^2_{q\bar{q} \to q'\bar{q}'}(t,s,u)$$

since we make the exchange $q \leftrightarrow q'$**,** $p_2 \leftrightarrow -p_3$ **or** $s \leftrightarrow t$**.**

Exercise: find expressions for $\sum |M|^2_{q\bar{q} \to gg}$ **and** $\sum |M|^2_{gg \to q\bar{q}}$

Spin averaged lowest order matrix elements

In fact, all of the various matrix elements have very similar shape. we see that

$$\sum |M|^2_{gq\to gq} + \sum |M|^2_{gq\to qg}$$
$$\sim \frac{4}{9}\sum |M|^2_{gg\to gg}$$

and similarly for quark initiated processes

$\Rightarrow$ **The single effective subprocess**

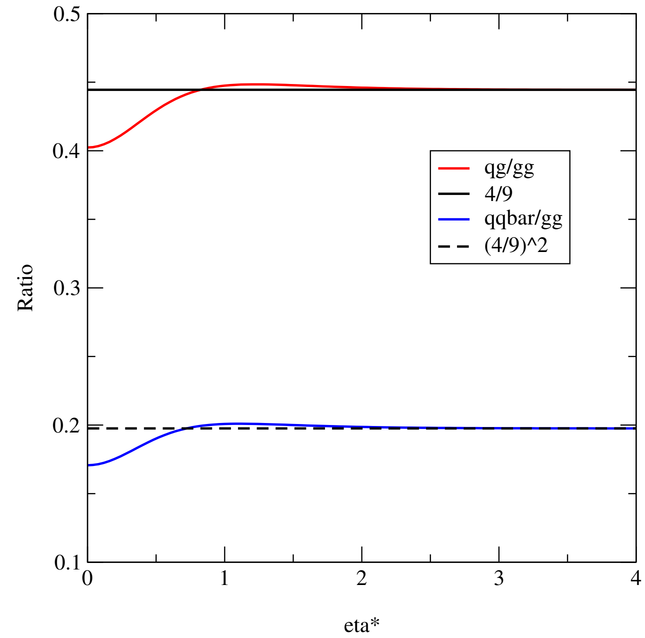

Ratios of matrix elements for qg/gg and $q\bar{q}/gg$ as a function of the centre-of-mass rapidity η^*

The single effective subprocess

Can write the lowest order cross section approximately as

$$\frac{d^3\sigma}{dE_T d\eta_1 d\eta_2} \sim \frac{1}{8\pi}\, x_1 F(x_1,\mu_F)\, x_2 F(x_2,\mu_F) \times \frac{\alpha_s^2(\mu_R)}{E_T^3}\,\frac{|\mathcal{M}_{gg\to gg}|^2}{\cosh^4\eta^*},$$

where $F(x,\mu)$ is the **single effective parton density**,

$$F(x,\mu) = g(x,\mu) + \frac{4}{9}\sum_q \left(q(x,\mu) + \bar{q}(x,\mu)\right).$$

The sum over parton subprocesses is accounted for by $F(x,\mu)$.

$\Rightarrow$ Can understand jet cross sections at lowest order in terms of

- ✓ Gluonic matrix elements
- ✓ $F(x,\mu)$

Gluonic matrix elements

The parton-parton sub-process scattering matrix elements are independent of η^{boost} so the only variation is with the centre-of-mass rapidity η^*,

$$\frac{|\mathcal{M}_{gg\to gg}|^2}{\cosh^4(\eta^*)} = \frac{9\pi^2}{8}\frac{(4\cosh^2(\eta^*)-1)^3}{\cosh^6(\eta^*)}.$$

As $|\eta^*|$ gets large, t (or u) $\to 0$ and we approach the regge limit.

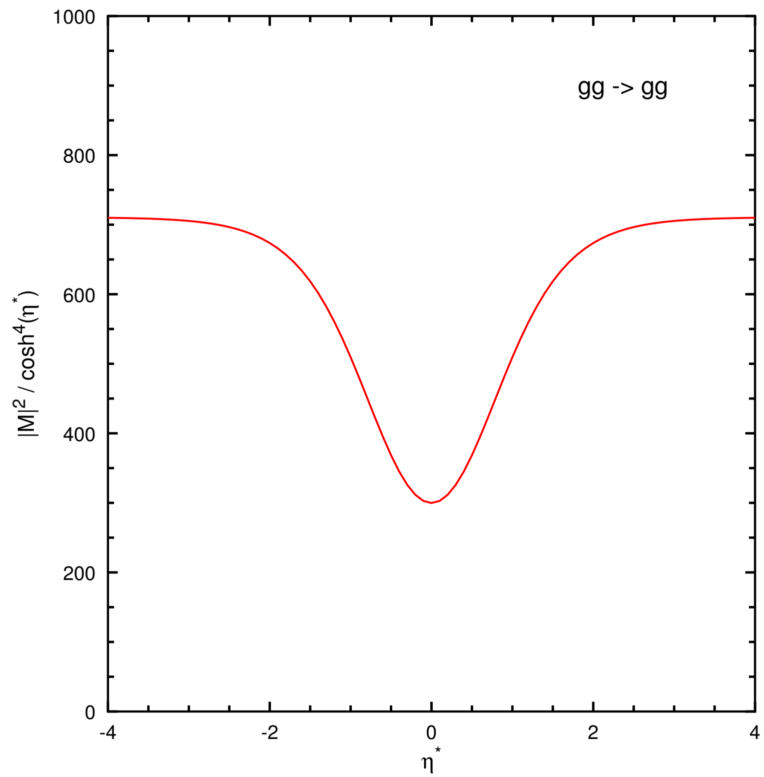

Parton luminosity

The parton-parton luminosity in the single effective subprocess approximation as a function of $\eta^{\rm boost}$ for different $|\eta^*|$ values ($E_T = 100$ GeV and $\sqrt{s} = 2$TeV). This corresponds to diagonal strips across the $\eta_1 - \eta_2$ plane.

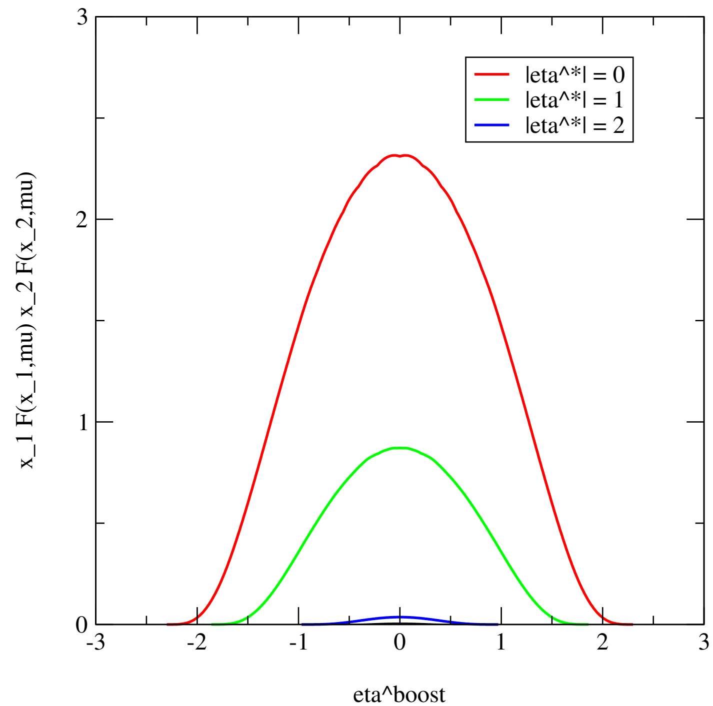

As expected, the largest luminosity occurs when x_1 and x_2 are equally small, $\eta^* \sim \eta^{\rm boost} = 0$. As either $|\eta^{\rm boost}|$ or $|\eta^*|$ increases, the luminosity decreases rapidly. However the falloff is more rapid with increasing $|\eta^*|$ than with increasing $|\eta^{\rm boost}|$.

The unphysical scales - μ_R

The **renormalisation scale** μ_R is introduced when redefining the bare fields in terms of the physical fields at scale μ_R. It is unphysical - and the answer shouldnt depend on it - but does because we work at a fixed order in perturbation theory. Therefore, you can choose any value (within reason). Typical values are the hard scale in the process $\mu_R \sim E_T$.

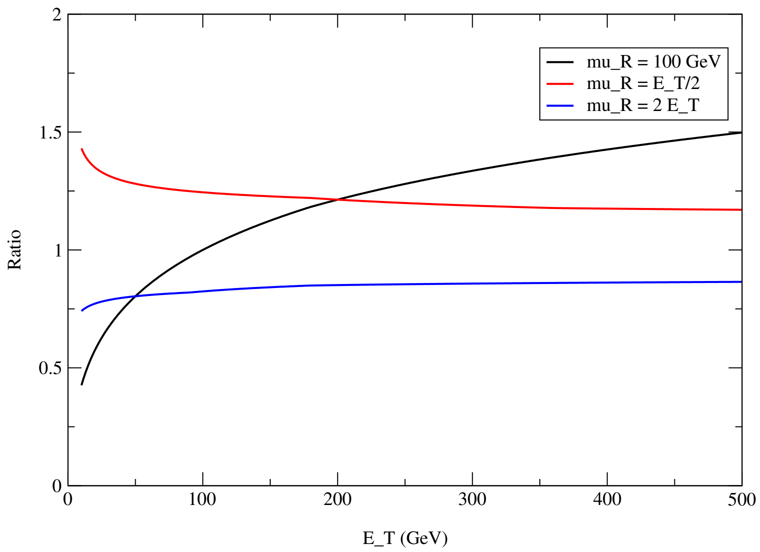

α_s^2 for various values of μ_R compared to $\mu_R = E_T$

The unphysical scales - μ_F

The **factorisation scale** μ_F is introduced when absorbing the divergence from collinear radiation into the parton densities. It is unphysical - and the answer shouldnt depend on it - but does because we work at a fixed order in perturbation theory. Typically, we think of radiation at a transverse scale $> \mu_F$ as being detectable so that $\mu_F \sim E_T$ is a reasonable choice.

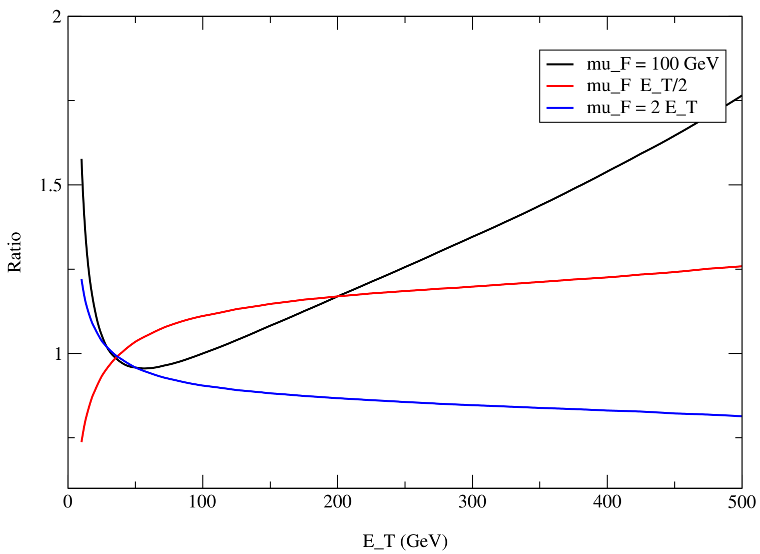

The effective parton-parton luminosities for various values of μ_F compared to $\mu_F = E_T$ at $\eta_1 = \eta_2 = 0$

Gluon v Quark contribution

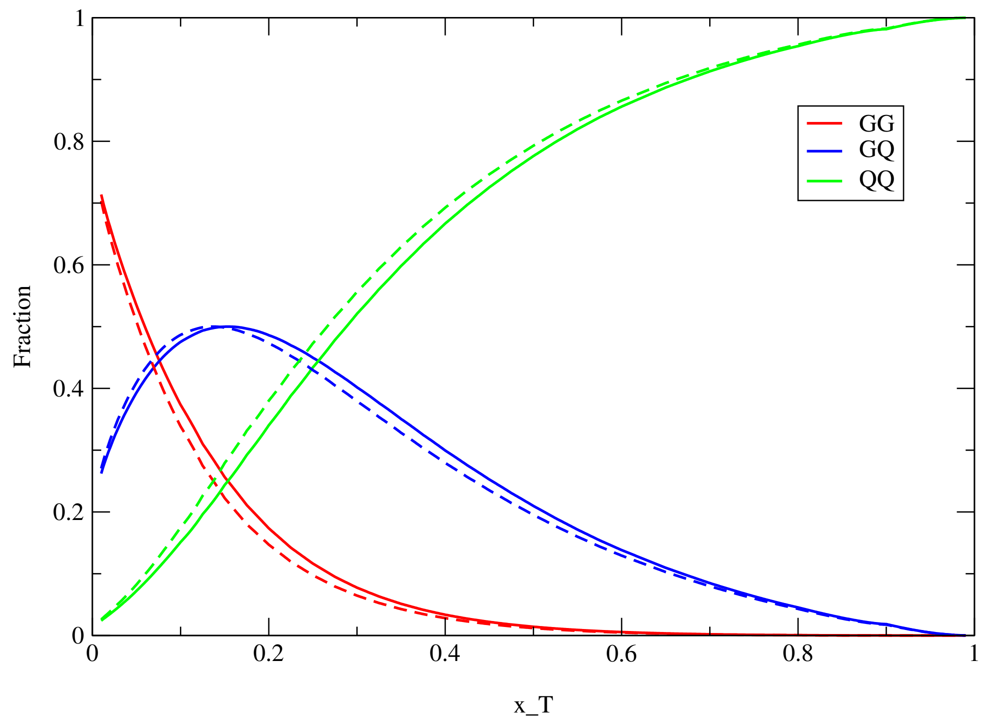

Fraction of cross section from gluon-gluon, gluon-quark and quark-quark processes at $\eta_1 = \eta_2 = 0$ at $\sqrt{s} = 2$ TeV (solid) and $\sqrt{s} = 14$ TeV (dashed) $x_T = 2E_T/\sqrt{s}$
Mostly gluon initial state at low x_T and quark initiated at large x_T.
At $x_T \sim 0.5$, gluons responsible for 20% of cross section.

Scaling cross section

The scaled cross section is independent of $\sqrt{s}$

$$E_T^3 \frac{d^3\sigma}{dE_T d\eta_1 d\eta_2} \sim \frac{1}{8\pi} x_1 F(x_1, \mu_F)\, x_2 F(x_2, \mu_F)$$

$$\times \quad \alpha_s^2(\mu_R) \frac{|\mathcal{M}_{gg\to gg}|^2}{\cosh^4 \eta^*}$$

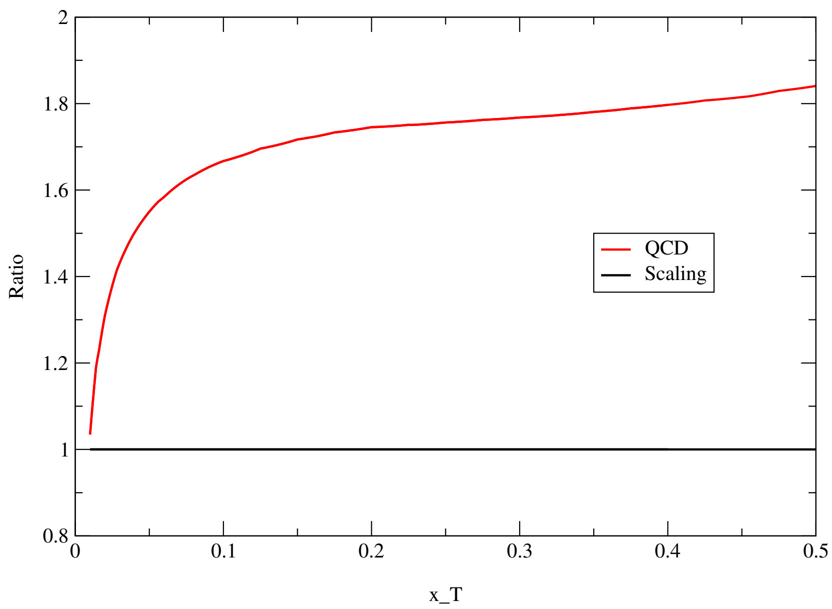

Ratio of $E_T^3 d^3\sigma/dE_T/d\eta_1/d\eta_2$ **at** $\eta_1 = \eta_2 = 0$ **for** $\sqrt{s} = 630$ **GeV and** $\sqrt{s} = 1800$ **GeV versus** $x_T = 2E_T/\sqrt{s}$**.**

Scaling violations due to strong coupling and evolution of parton densities.

Dijet angular distribution

Can also work in terms of the dijet mass M_{JJ} and the centre-of-mass scattering angle θ^*

$$M_{JJ}^2 = 4E_T^2 \cosh^2 \eta^*, \qquad \cos\theta^* = \tanh \eta^*, \qquad t = -\frac{s}{2}(1-\cos\theta^*)$$

$$\frac{d^3\sigma}{dM_{JJ}^2 d\cos\theta^*} \sim \int dx_1 dx_2 F(x_1,\mu_F)\, F(x_2,\mu_F)\, \delta(x_1 x_2 s - M_{JJ}^2)$$

$$\times \quad \frac{\alpha_s^2(\mu_R)}{32\pi M_{JJ}^2} |\mathcal{M}_{gg\to gg}|^2$$

at small t (large $\cos\theta^*$)

$$|\mathcal{M}_{gg\to gg}|^2 \sim \left(\frac{s}{t}\right)^2 \sim \frac{1}{(1-\cos\theta^*)^2},$$

the classic Rutherford scattering behaviour for the exchange of a massless vector boson in the t-channel.

Dijet angular distribution

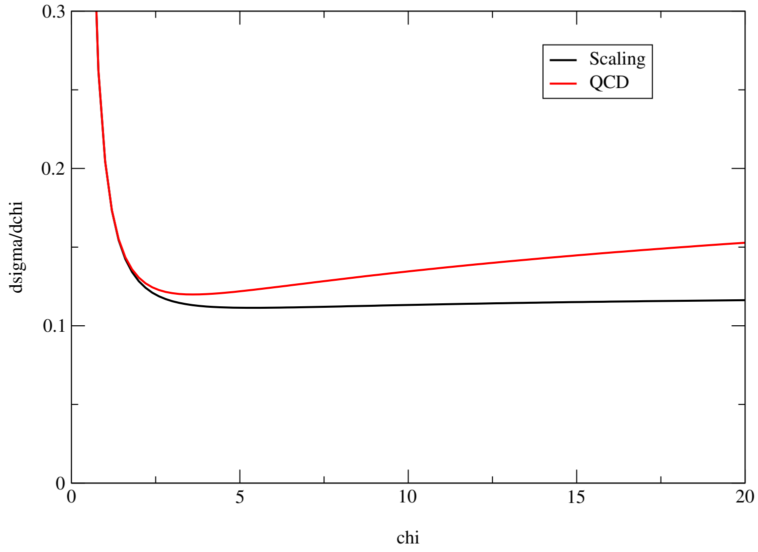

$d\sigma/d\chi$ **for** $M_{JJ} = 200$ **GeV,** $\eta^{\rm boost} = 0$ **and** $\sqrt{s} = 2$ **TeV.**

An even better variable is

$$\chi = e^{2\eta^*} = \left(\frac{1+\cos\theta^*}{1-\cos\theta^*}\right)$$

that removes the singular behaviour as $t \longrightarrow 0$, $\cos\theta^* \longrightarrow 1$

Scaling violations due to strong coupling and evolution of parton densities.

Jet algorithms

So far, at leading order the jet is represented by a single parton.

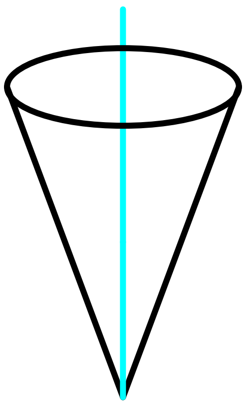

$\Rightarrow$ it doesnt matter what the jet definition is... (unless we deal with multiparton configurations and we want to separate the partons)
$\Rightarrow$ motivations for higher order corrections are to

- improve the matching between theoretical and experimental jets
- reduce the dependence on the unphysical scales
- identify kinematic regions where logarithms are large
- model radiation outside of the jet

Structure of NLO

Example, pure gluon ingredients to $pp \longrightarrow 2$ jets

- 1 loop, 2 parton final state

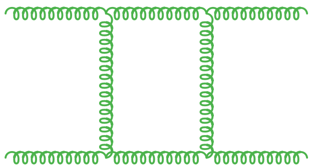

Same kinematics as leading order - single parton $\equiv$ jet

- tree level, 3 parton final states
  or 2+1 parton final state

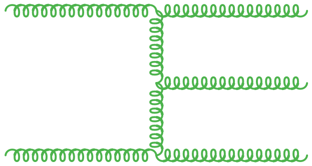

Different kinematics - extended phase space and now have the possibility of partons combining to form jet

$\Rightarrow$ sensitivity to jet algorithm
- size of jet and way in which momenta are combined

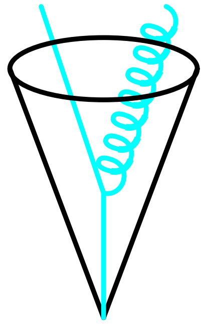

NLO phase space

- The parton fractions are given by

$$x_{1,2} = \frac{E_{T1}}{\sqrt{s}} \left(\exp(\pm\eta_1) + \frac{E_{T2}}{E_{T1}} \exp(\pm\eta_2) + \frac{E_{T3}}{E_{T1}} \exp(\pm\eta_3) \right),$$

  where $E_{T1} > E_{T2} \geq E_{T3}$.

- Since the transverse energies of the partons are no longer forced to be equal, $|\eta_2|$ may increase to compensate for having a smaller transverse energy,
$E_{T2}/E_{T1} < 1$.

- The maximum possible values of $|\eta_2|$ occur when $E_{T2} = E_{T3}$,

$$-\log\left(\frac{a\bar{a} + \sqrt{a^2\bar{a}^2 - a\bar{a}}}{a}\right) < \eta_2 < \log\left(\frac{a\bar{a} + \sqrt{a^2\bar{a}^2 - a\bar{a}}}{\bar{a}}\right),$$

  where

$$a = \frac{(2 - x_{T1}\exp(\eta_1))}{x_{T1}} \qquad \bar{a} = \frac{(2 - x_{T1}\exp(-\eta_1))}{x_{T1}}$$

NLO phase space

- The maximum allowed value of $|\eta_1|$ is unchanged at next-to-leading order
- Adding more partons into the final state further increases the allowed η_2 range corresponding to the production of more and more soft partons.
- The physical cross section will exhibit a rather sharp cutoff as $|\eta_1|$ increases.
- There will be a more gradual fall off in the cross section as $|\eta_2|$ increases.

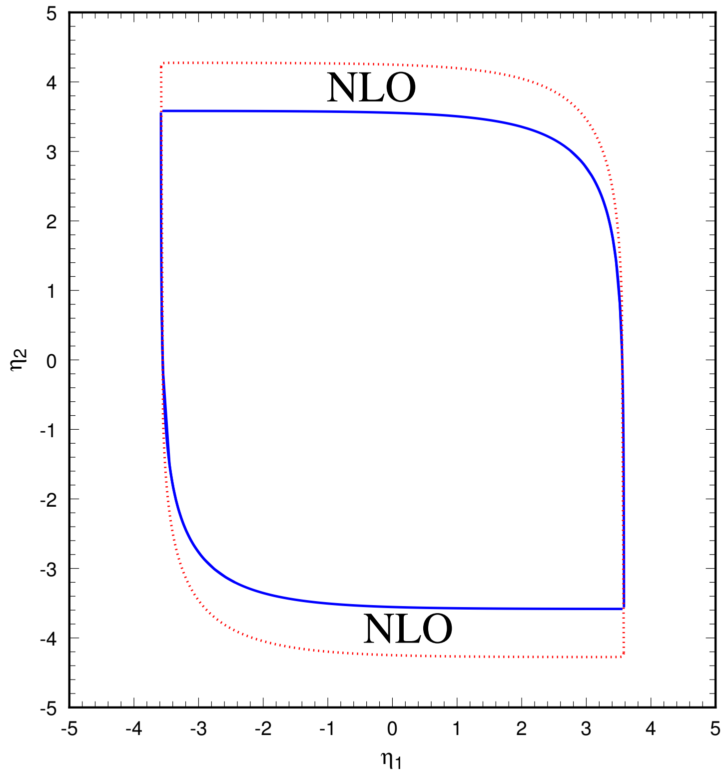

Phase space for $E_T = 50$ GeV and $\sqrt{s} = 1.8$ TeV.

NLO matrix elements

The matrix elements for

$$a(p_1) + b(p_2) \to c(p_3) + d(p_4) + e(p_5)$$

averaged (summed) over initial (final) state colours and spins are

$$|\mathcal{M}_{qq' \to qq'g}|^2 = \frac{4}{9} g^6 \left(\frac{s^2 + s'^2 + u^2 + u'^2}{tt'} \right)$$
$$\times \quad \left(2C_F \left([14] + [23] \right) + \frac{1}{N} \left(2[12] + 2[34] - [13] - [14] - [23] - [24] \right) \right)$$

where (since $p_5 \neq 0$) the primed and unprimed variables are different

$$\begin{aligned} s &= (p_1 + p_2)^2, \qquad t = (p_1 - p_3)^2, \qquad u = (p_2 - p_3)^2 \\ s' &= (p_3 + p_4)^2, \qquad t' = (p_2 - p_4)^2, \qquad u' = (p_1 - p_4)^2 \end{aligned}$$

and the eikonal factor

$$[ij] = \frac{p_i . p_j}{p_i . p_5 \; p_5 . p_j}$$

accounts for the coherent radiation of gluons from the quarks

NLO matrix elements

In the limit that the gluon is either soft ($p_5 \to 0$) or collinear with one of the quarks, the matrix element factorises

$$|\mathcal{M}_{qq' \to qq'g}|^2 \to |\mathcal{M}_{qq' \to qq'}|^2 X$$

where X is a factor that contains the infrared singular terms and

$$|\mathcal{M}_{qq' \to qq'}|^2 = \frac{4}{9} g^4 \left(\frac{u^2 + s^2}{t^2} \right)$$

For example, in the soft limit $s' \to s$, $t' \to t$ and $u' \to u$ so that by trivial inspection,

$$X = 2g^2 \left\{ 2C_F \left([14] + [23] \right) + \frac{1}{N} \left(2[12] + 2[34] - [13] - [14] - [23] - [24] \right) \right\}$$

with the eikonal factor $[ij] = p_i.p_j / p_i.p_5 \; p_5.p_j$ diverging in the $p_5 \to 0$ limit.

Soft factors like this dictate all **interjet coherence** phenomena

Exercise

In the limit where p_4 and p_5 are **collinear** (so $p_4.p_5 \to 0$), make the replacements

$$p_4 = (1-z)p_{45}, \qquad p_5 = z\, p_{45}$$

so that

$$s' = 2p_3.p_4 \to (1-z)2p_3.p_{45} = (1-z)s$$

etc and

$$[i4] = \frac{p_i.p_4}{p_i.p_5\; p_4.p_5} \to \frac{(1-z)p_i.p_{45}}{zp_i.p_{45}\; p_4.p_5} = \frac{1-z}{z}\,\frac{1}{p_4.p_5}.$$

Hence show that

$$|\mathcal{M}_{qq'\to qq'g}|^2 \to |\mathcal{M}_{qq'\to qq'}|^2 X$$

where (ignoring terms that do not diverge in the collinear limit)

$$X = C_F g^2 \,\frac{4}{p_4.p_5}\,\frac{1+(1-z)^2}{z}$$

— the splitting function for a quark to radiate a collinear gluon.

Overall effect of NLO corrections

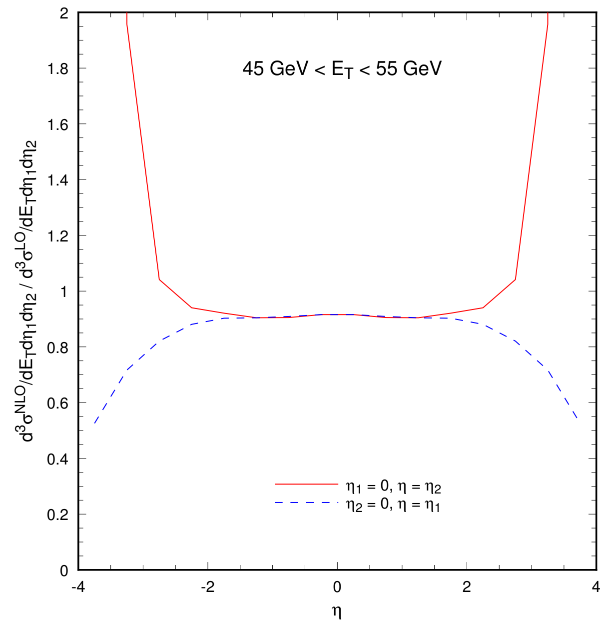

K-factor for $E_T = 45 - 55$ GeV and $\sqrt{s} = 1.8$ TeV

Moderate corrections away from phase space boundaries - identify large logarithmic corrections at large $\eta_2 \Rightarrow$ resummation.

Jet algorithm

Must be infrared safe:

- Infrared problem - adding an infinitely soft parton should not change the number of jets

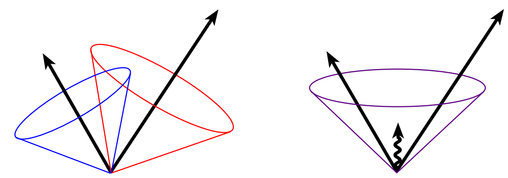

- Collinear problem - replacing any massless parton with an exactly collinear pair of massless partons should not change the number of jets

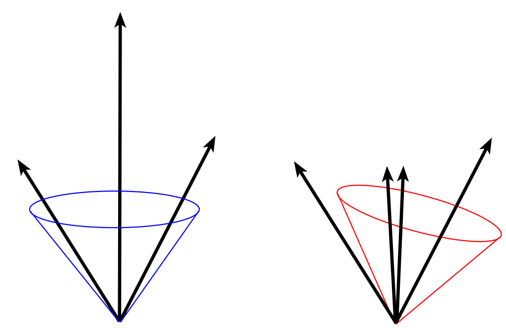

+ insensitive to hadronisation
+ insensitive to longitudinal boosts
+ simple to apply to higher orders and experiment

Jet definitions

The transverse energy, E_T, pseudorapidity, η, and azimuth, ϕ, of a jet are given by:

$$
\begin{aligned}
E_{T\mathrm{jet}} &= \sum_{i\in\mathrm{jet}} E_{Ti}\,, \\
\eta_{\mathrm{jet}} &= \sum_{i\in\mathrm{jet}} E_{Ti}\,\eta_i / E_{T\mathrm{jet}}\,, \\
\phi_{\mathrm{jet}} &= \sum_{i\in\mathrm{jet}} E_{Ti}\,\phi_i / E_{T\mathrm{jet}}\,.
\end{aligned}
$$

We shall always use boost-invariant variables, so 'angle'means the Lorentz-invariant opening angle

$$R_{ij} = \sqrt{(\eta_i - \eta_j)^2 + (\phi_i - \phi_j)^2}$$

k_T algorithm

- For every pair of particles, define a closeness

$$d_{ij} = \min(E_{Ti}, E_{Tj})^2 R_{ij}^2 \left(\approx \min(E_i, E_j)^2 \theta_{ij}^2 \approx k_\perp^2\right).$$

- For every particle, define a closeness to the beam particles,

$$d_{ib} = E_{Ti}^2 R^2.$$

- If $\min\{d_{ij}\} < \min\{d_{ib}\}$, **merge** particles i and j
- If $\min\{d_{ib}\} < \min\{d_{ij}\}$, jet i is **complete**.

These steps are iterated until all jets are complete. In this case, all opening angles within each jet are $< R$ and all opening angles between jets are $> R$.
Note: not every particle within R of the jet axis is included - the cone has a **flexible** edge.

Cone algorithm

- For every seed tower sum all cells within angle R
- Recompute jet direction and iterate until stable jet direction found
- If jets overlap, **merge** and **split** jet

Note that despite the use of a fixed cone of radius R, jets can contain energy at angles greater than R from their direction, because of merging procedure.

- At the **NLO parton level**, sometimes require that the two partons must be within $R_{\rm sep} R$ of each other — this is **ad hoc** parameter not present in experimental algorithm.
- Midpoint or **improved legacy cone algorithm** – pseudo-seed towers placed midway between jets with $R < \Delta R < 2R$ corresponds to $R_{\rm sep} = 2$.
- k_T-algorithm corresponds to $R_{\rm sep} = 1$.

The single jet inclusive cross section

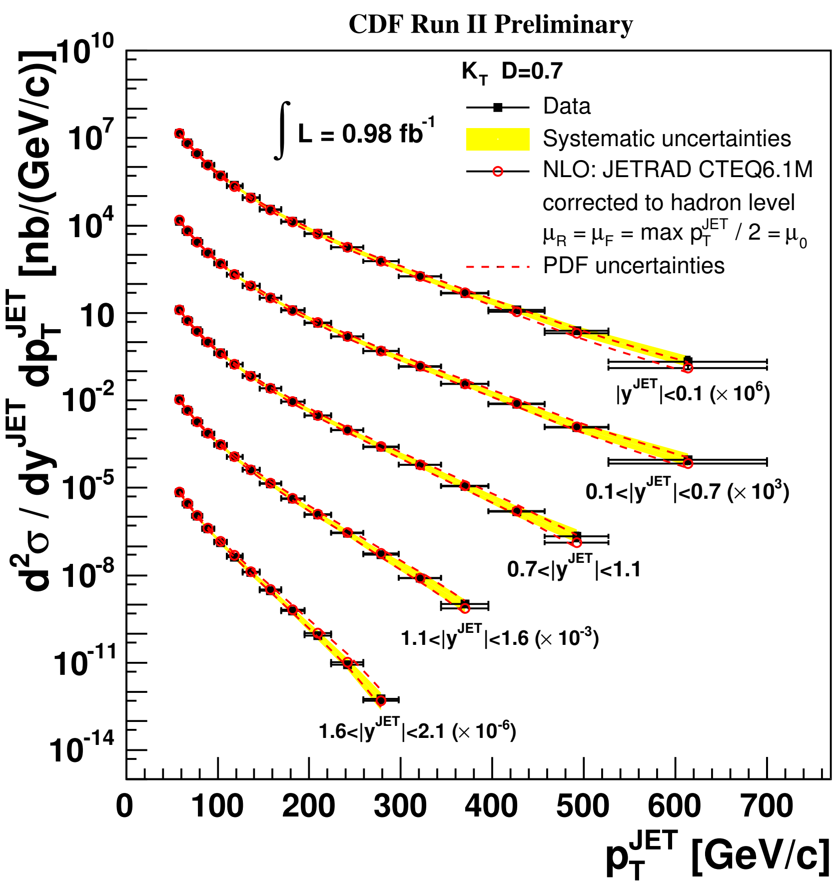

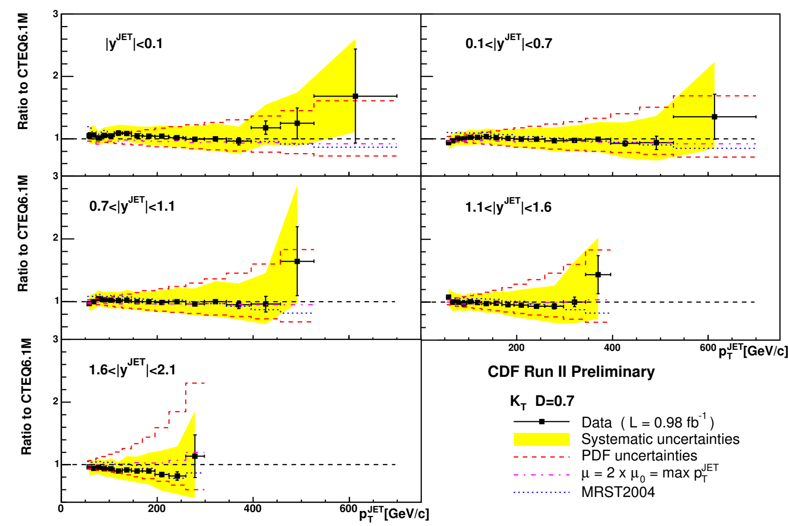

K_T algorithm

Excellent agreement with NLO QCD + CTEQ6.1

At LHC will probe to 4TeV

The single jet inclusive cross section

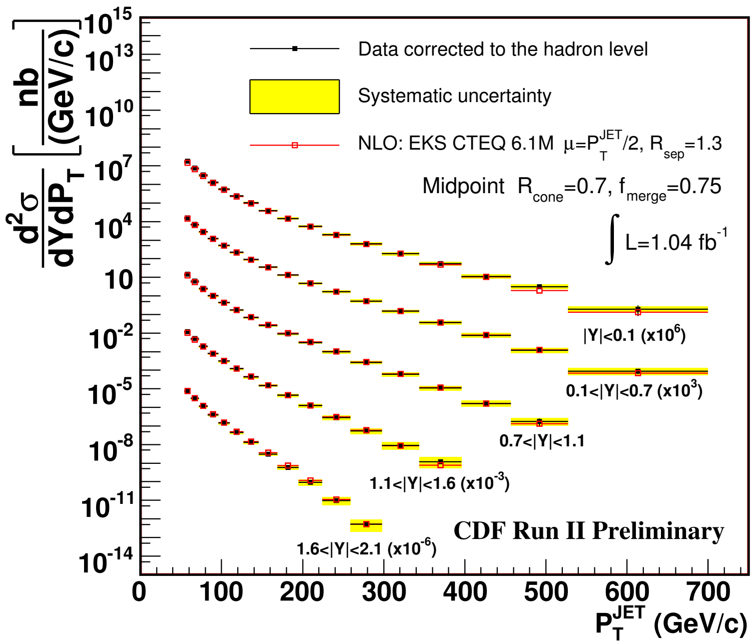

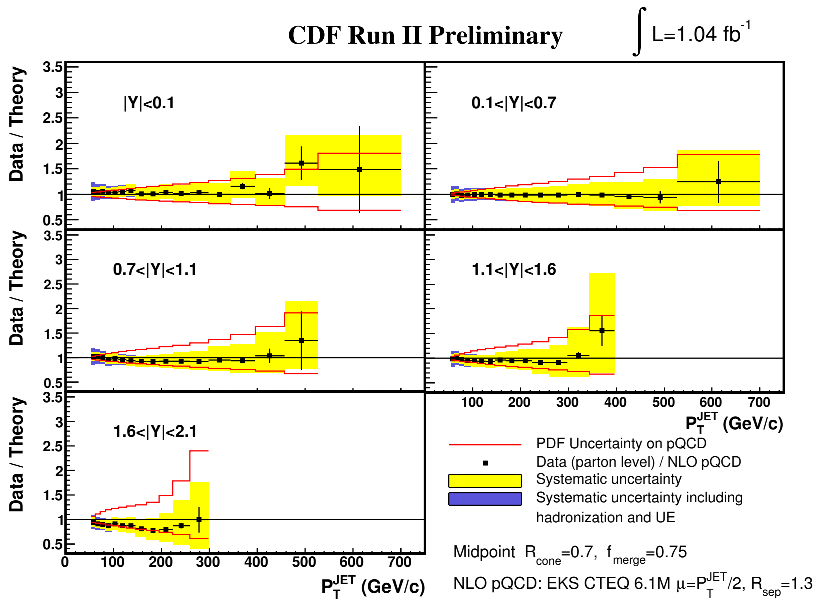

cone algorithm

Excellent agreement with NLO QCD + CTEQ6.1

At LHC will probe to 4TeV

Scaling cross section

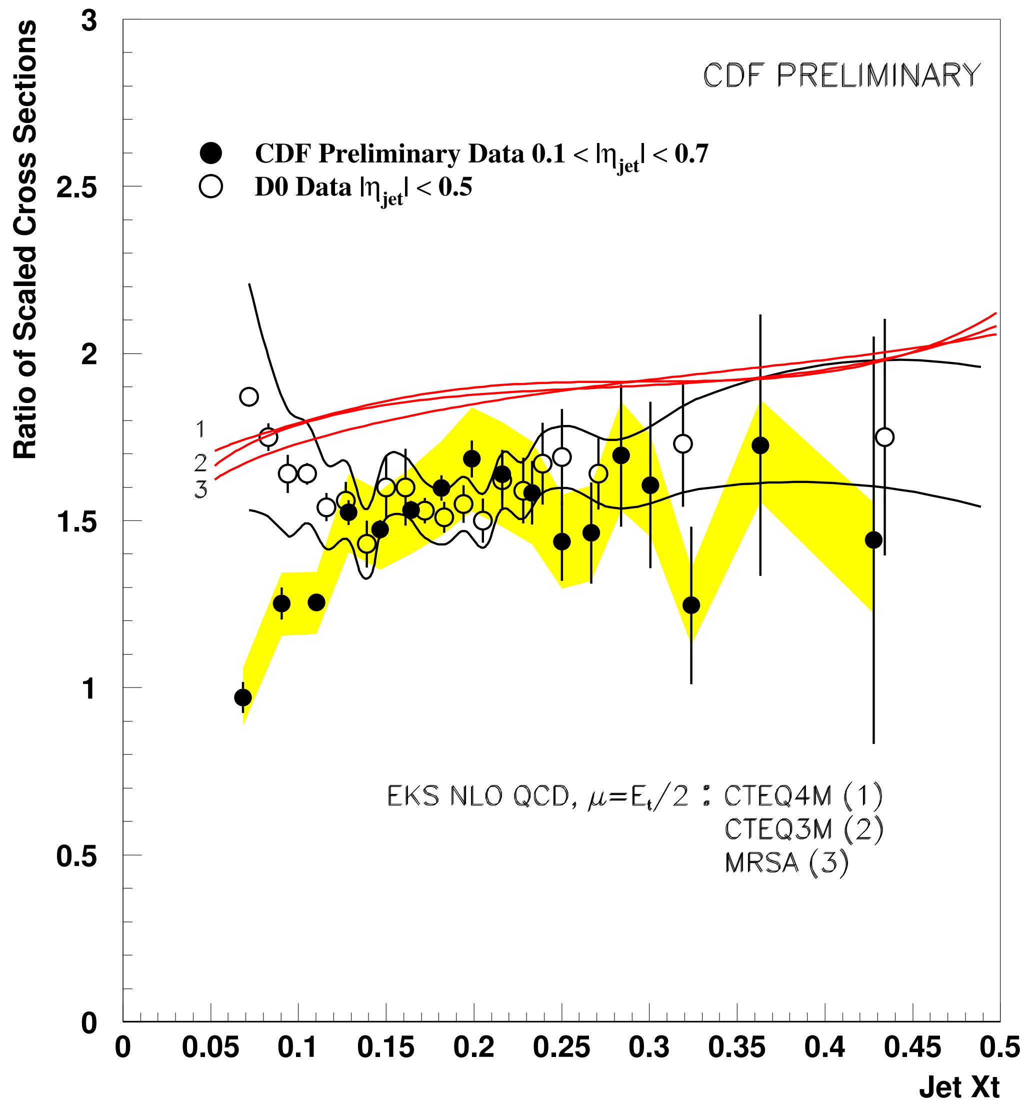

Dijet angular distribution

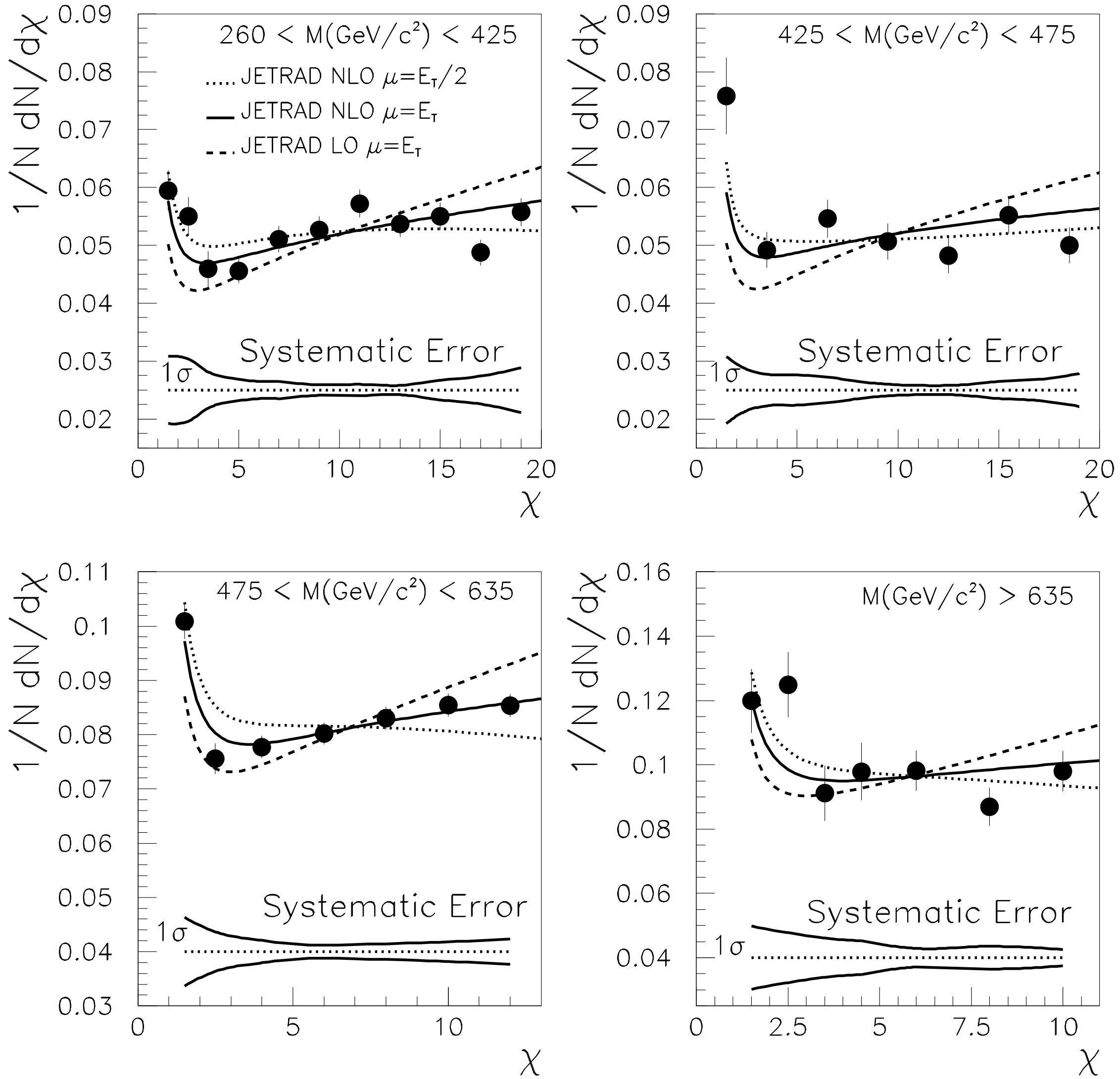

Jet shape

The jet shape can be defined as

$$\Psi(r;R) = \frac{\sum_i E_{Ti}\Theta(r - R_{ijet})}{\sum_i E_{Ti}\Theta(R - R_{ijet})}$$

where the sum is over the particles in the jet.

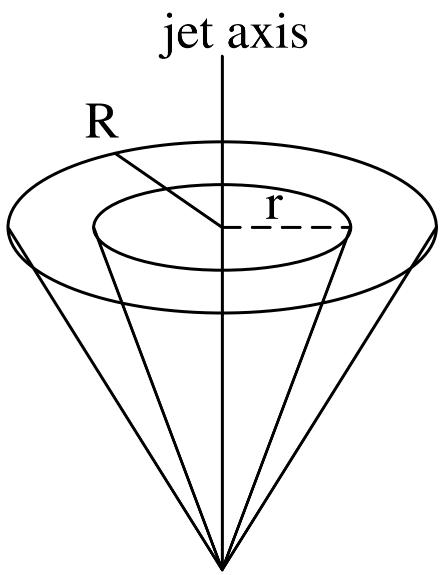

Ψ is the fraction of energy of a jet of size R contained in a sub-cone of size r so that

$$\Psi(R;R) = 1$$

Differential jet shape weighted by r

$$\rho(r,R) = \frac{d\Psi(r,R)}{dr}$$

Jet shape cont'd

There are two (perturbative) contributions

- Radiation inside the jet
  modelled by collinear splitting

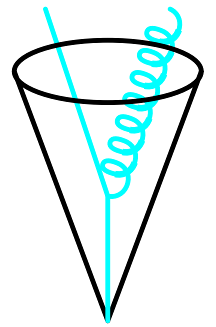

- Soft gluons falling into the cone
  modelled by coherent soft radiation pattern

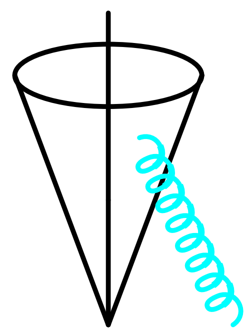

Radiation in jet

The probability of final-state emission from a parton of type a

$$dP_a = \frac{1}{2}\sum_b \frac{\alpha_s}{2\pi}\frac{d\theta^2}{\theta^2}\, dz\, P_{a\to bc}(z),$$

where z is the fraction of a's energy carried by b, and θ is the opening angle between the partons.
The phase space limits come from the requirements that both partons be within R of the jet axis, and the opening angle be less than $R_{\rm sep}R$.
Doing the integration over z, we find for quark and gluon jets

Seymour hep-ph/9707338

$$\begin{aligned} r\rho_q(r) &= \frac{C_F\alpha_s}{2\pi}\left[2\left(-2\log Z - \frac{3}{2}(1-Z)^2\right)\right], \\ r\rho_g(r) &= \frac{C_A\alpha_s}{2\pi}\left[2\left(-2\log Z - (1-Z)^2\left(\frac{11}{6} - \frac{1}{3}Z + \frac{1}{2}Z^2\right)\right)\right] \\ &+ \frac{T_R N_f \alpha_s}{2\pi}\left[2(1-Z)^2\left(\frac{2}{3} - \frac{2}{3}Z + Z^2\right)\right], \end{aligned}$$

$Z = r/(r+R)$ if $r < (R_{\rm sep}-1)R$ and $Z = r/R_{\rm sep}R$ otherwise

Soft radiation from outside the jet

This is due to soft initial-state radiation that happens to be inside the jet cone by chance,

$$dP = 4\frac{C\alpha_s}{2\pi}\, d\eta\, \frac{d\omega}{\omega} \sim 4\frac{C\alpha_s}{2\pi}\, \theta d\theta\, \frac{dz}{z}$$

with colour factor $C \sim C_F \sim C_A/2$.
Applying the phase space limits gives

$$r\rho_i(r) = \frac{C\alpha_s}{2\pi}\left[2r\left(\frac{1}{Z^2} - 1\right)\right].$$

Initial radiation is insensitive to the jet direction, but this still gives a finite contribution as $r \rightarrow 0$. This is due to the fact that soft partons anywhere in the jet will pull the jet axis away from the hard parton direction.
Note: we are making small angle approximations so these simple formulae will make an error at large values of R and R_{sep}.

Shape of jet

Also expect **power corrections** and **large infrared logarithms**

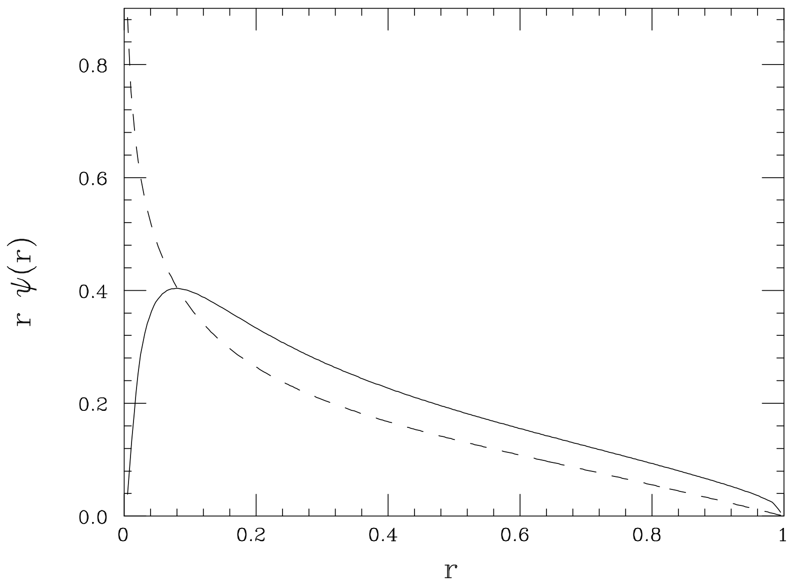

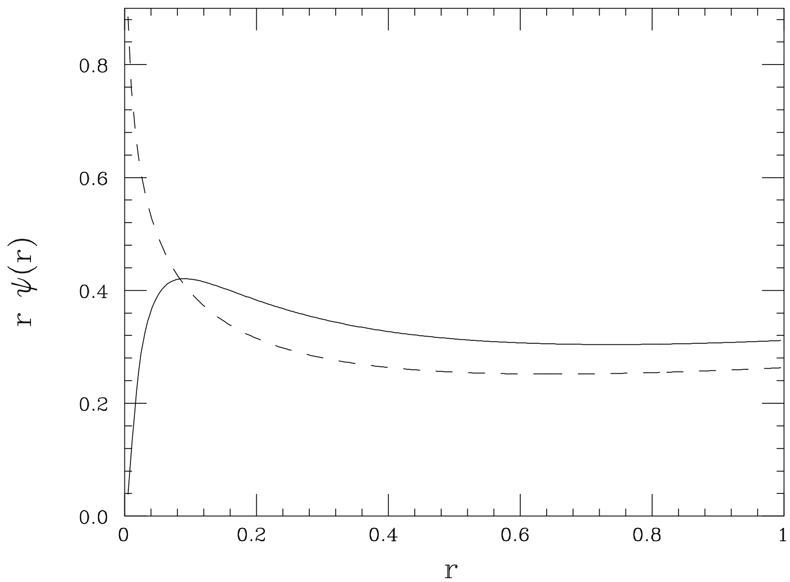

K_T **algorithm** — $R = 1$, $R_{\mathrm{sep}} = 1$.

cone algorithm — $R = 1$, $R_{\mathrm{sep}} = 2$

The solid line is the resummed result including power corrections.

Seymour hep-ph/9707338

Shape of jet

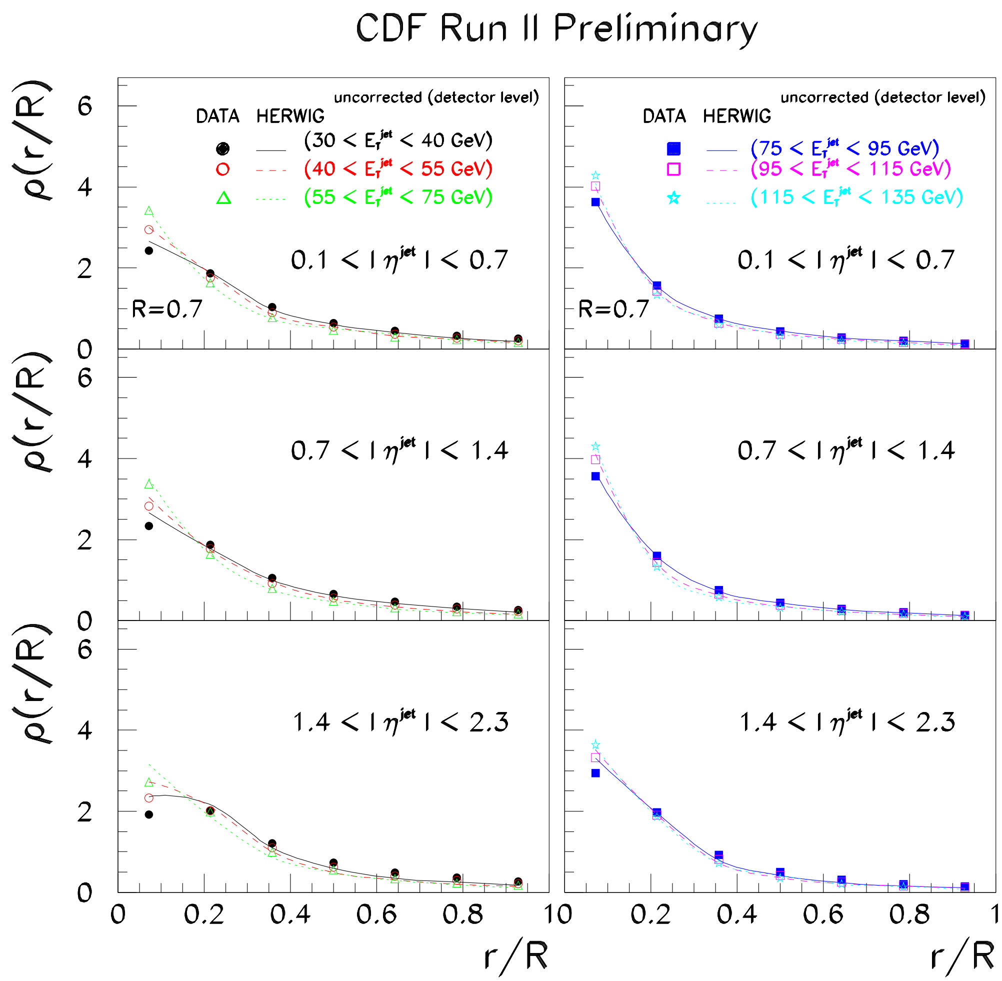

CDF Run II Preliminary
uncorrected (detector level)
DATA HERWIG
(30 < E_T^{jet} < 40 GeV)
(40 < E_T^{jet} < 55 GeV)
(55 < E_T^{jet} < 75 GeV)
(75 < E_T^{jet} < 95 GeV)
(95 < E_T^{jet} < 115 GeV)
(115 < E_T^{jet} < 135 GeV)
0.1 < | η^{jet} | < 0.7
0.7 < | η^{jet} | < 1.4
1.4 < | η^{jet} | < 2.3
R=0.7
$\rho(r/R)$
r/R

Summary

- ✓ Jet physics is extremely rich field with diverse phenomena
- ✓ focussed on single and dijet production at high energies
  $\Rightarrow$ probing QCD to $\sim$few 10^{-18} m ($\sim$few 10^{-19} m at LHC)
- ✗ didn't have time for
  - multijet events
  - vector boson(s) + jets
  - heavy flavour jets
  - diffractive jet production
  - multiple parton scattering
  - $\ldots$
- ✓ Understanding jet physics is **key** to understanding photons, leptons, missing transverse energy
  $\Rightarrow$ possible discovery on phenomena beyond the Standard Model